



## Optical Properties of CuInTe<sub>2</sub> Single Crystals by Photoacoustic Spectroscopy

A. Bouloufa, A. Messous, M.V. Yakushev\*, R.D. Tomlinson\* and A. Zegadi

Laboratoire: Croissance et Caractérisation de Nouveaux Semiconducteurs.

Département d'Electronique, Faculté des Sciences de l'Ingénieur, Université Ferhat Abbas - Sétif,  
Sétif 19000, Algeria. Telefax: +213 36 92 51 27. e-mail : [Abdeslam\\_bouloufa@yahoo.fr](mailto:Abdeslam_bouloufa@yahoo.fr)

\*Physics Department, University of Salford, Salford M5 4WT, UK.

### Abstract –

This paper reports on the optical properties of the photovoltaic material CuInTe<sub>2</sub> (CIT) as characterised by photoacoustic spectroscopy (PAS). Measured spectra of p-conducting CIT single crystals are given using a high resolution photoacoustic spectrometer of the gas-microphone type. The data is used to evaluate the absorption spectra, the band gap energy, and ionisation energies of defects that have been observed in the tail of the spectra. The obtained Results confirm the efficiency of the technique in detecting the non-radiative defects known to dominate the properties of this compound. A discussion on the relation between the composition of the samples and the intrinsic defect chemistry in this compound is also given. Finally, we give a comparison between the results we have obtained and those published in the literature.

**Key words:** CuInTe<sub>2</sub>; Optical properties, Photoacoustic spectroscopy, Defect chemistry.

### INTRODUCTION

The ternary compounds type A<sup>I</sup>B<sup>III</sup>C<sub>2</sub><sup>VI</sup> which belong to the family of chalcopyrite semiconductors have received considerable attention in recent years due to their potential applications in domains such optoelectronic devices, and solar cells[1-3]. However, despite the significant efforts devoted to improve the efficiency of devices based on these materials, this remains limited by the fact that the preparation of these materials with desirable electrical and optical properties is difficult because of the complex intrinsic defect structure of these compounds [4-6].

The influence of growth parameters and the subsequent etch conditions on the electrical properties of A<sup>I</sup>B<sup>III</sup>C<sub>2</sub><sup>VI</sup> have been published in the literature [5]. However, There is no definite model through which the experimental results can be interpreted in the appropriate manner. In particular, the identification of the electrically active intrinsic defect remains an open question.

CuInSe<sub>2</sub>, CuInS<sub>2</sub>, and CuInTe<sub>2</sub> are actually attracting an increasing attention in the field of optoelectronic devices. For Example, thin film solar cell employing Cu(In,Ga)Se<sub>2</sub> (CIGS) – based absorber layers have achieved efficiencies in excess of 19% [1]. It is suggested that solar cells based on CIT as the absorber layer having a band gap around 1eV (at room temperature) which is near that of CuInSe<sub>2</sub> should give the same order of efficiency [7], yet this is not the case.

Thin films of CIT can be obtained n or p conducting depending on the preparation conditions. However, when grown in single crystal ingots, the compound is always found p-conducting. Several researchers have attempted to change the conductivity type of single crystals but have failed. Its band gap energy E<sub>g</sub> has been determined using several measurement techniques. It has been shown that this one lies in a large interval. This is due to the fact that this compound comes originally heavily doped [5].

Photoacoustic spectroscopy (PAS) is a newly developed measurement technique that yields important information on the absorption of semiconductors. PAS yields direct information on non-radiative absorption processes which are usually associated with the band structure and defect-related energy loss mechanisms. Such information is essential for materials which could find applications in electronic devices [8-11].

In this paper, a high resolution near infrared photoacoustic spectrometer of the gas-microphone type is used to study the non-radiative defect structure of CIT at room temperature. Photoacoustic (PA) spectra are measured near the fundamental absorption edge of as-grown CuInTe<sub>2</sub> single crystals, grown from a near stoichiometric melt by the vertical Bridgman technique. The absorption coefficient and the gap energy are determined. Non-radiative defects observed on the absorption edges are discussed. A comparison between the results obtained here and published data is finally given.

### EXPERIMENTAL

The samples used in this work were all as-grown p-type conducting grown by using the vertical Bridgman technique[3]. Prior to being analysed, the samples were mechanically polished on both sides using a final 0.05µm grade Al<sub>2</sub>O<sub>3</sub> powder, then chemically etched in a 1% bromine in methanol solution for 1 minute, and finally rinsed in de-ionised water. This etch does not change the stoichiometry of the compound. The conductivity type of all the samples is determined using the thermal probe, and were found to be p-type conducting. The elemental composition, as determined by energy dispersive X-ray fluorescence spectroscopy has given for almost all the samples that we have analysed the following composition: Cu: 22.4%, In: 26.5%, Te: 51.1% with an estimated error of ±10%.

The optical properties (absorption coefficient spectra) are deduced from PA signals. The schematic diagram of the PA apparatus is shown in Fig. 1. In this diagram a Xenon short-arc lamp has been used as the radiation source. The light is chopped by a chopper at the frequency interval  $f=0.01-0.5\text{kHz}$ . An elliptic mirror concentrates the light on the sample in the photoacoustic cell. A infrared filter is placed between the monochromator and the elliptic mirror in order to suppress the scattered light. A Brookdeal lock-in amplifier amplifies the detected photoacoustic signal from the microphone. The output of the amplifier is read with a Keithley 175 auto-ranging digital voltmeter. A personal computer is used for the acquisition and the processing of PA data and to control the motor that drives the monochromator. The photoacoustic cell is cylindrical in shape containing the sample, the backing material, and the gas. The schematic picture of a gas-coupled PA cell is shown in Fig. 2. All theoretical studies predict that the amplitude of the PA signal detected by the microphone depends on the cell dimensions. In general, the signal increases with the reduction in the dimensions of the cell [11]. For this reason, the PA cell had to be specially designed. All spectra were recorded at room temperature in the photon energy range  $h\nu = 0.7$  to  $1.4$  eV. Finally, PA signal is corrected for the spectral distribution of the optical system and the cell by normalising the response of the sample to that of a fine powder of carbon black [11].

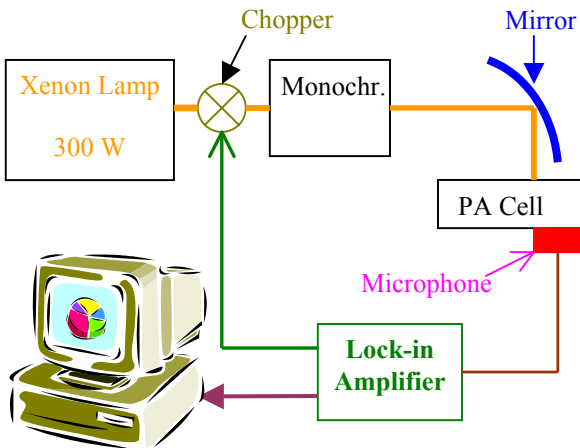


Fig. 1: Schematic diagram of the PA spectrometer.

**PHOTOACOUSTIC SPECTROSCOPY PRINCIPLE**

PAS is contact-less, non-destructive, and unique in observing non-radiative de-excitation processes and offer the potential for depth profiling analysis. These properties led to a widespread use of this technique in many domains.

The main mechanisms of the PA technique is the irradiation of a sample by sinusoidal chopped monochromatic light beam with a photon energy  $h\nu$ . The absorption of chopped light by samples is converted, in part or in whole, into heat by non-radiative de-excitation processes within the solid. This heat is generated inside of

the region between the illuminated surface and the layer under the surface. This one deduced a disruption of the temperature and the pressure on the superficial layer of the sample, that is detected by an acoustic or thermal mechanism or by the two. The produced signal is normalised and further processed using a personal computer.

Physically, the quantity of heat generated depends not only on the absorption and the efficiency of conversion coefficient of the material, but also of thermal diffusion coefficient of the material[8] given by the following formula:

$$\mu_s = \sqrt{\frac{2\kappa_s}{\omega C_s \rho_s}} \tag{1}$$

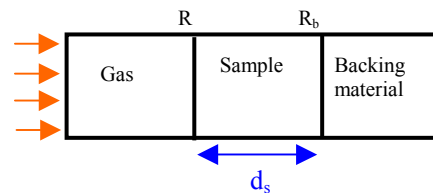


Fig.2 : Sectional view of PA cell.

where  $\kappa_s$  is the thermal conductivity,  $C_s$  is the specific heat and  $\rho_s$  is the density of the sample.  $\omega=2\pi f$  is the angular modulation frequency.

From (1), we can see that  $\mu_s$  depends on sample characteristics, on the modulation frequency of the light beam, on the parameters of the gas, and on the thermal conductivity of the sample. It decreases with increasing the modulation frequency. Coefficients of absorption and efficiency of the material in question give useful information on the expansion and the relaxation of the material. While, the thermal coefficient serves in the characterisation of the material (in measuring thermal properties of this material like the thermal diffusion and the thermal conductivity). The inconvenience remains the thermal and acoustic wave reflections by walls of the cell, notably in very elevated frequencies, what could produce interference and resonance phenomena inside the photoacoustic cell [11].

In the derivation of photoacoustic signal we suppose that any heat produced in the backing material does not have any influence on the signal [8-11], only if, the following condition is filled:

$$\mu_s < d_s \tag{2}$$

When  $d_s > \mu_s$ , the thermal wave is not attenuated greatly before having reached the limit gas-sample and the PA signal can be affected by the total energy absorbed in the sample. This means that the thickness of the sample is

an important factor in the interpretation of PA spectra. The gas layer adjacent to the surface of the semiconductor is shown in Fig. 3. From these curves we can see that waves are dumped after a certain distance. This means that only a thin limited layer that responds thermally to the excitation beam light. The variation of photoacoustic signal with the frequency of the light source is represented in Fig. 4. In this figure, we can clearly see that the PA signal reduces with increasing modulation frequency. The backing material can also affect the PA signal (see Fig.4). The sensitivity of the PA cell increases with increasing the reflection of the backing material.

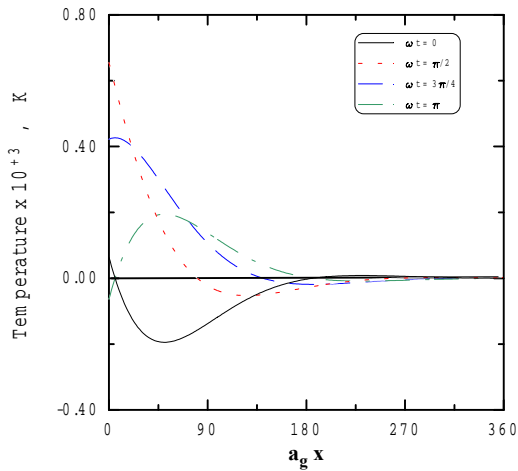


Fig. 3 : Spatial distribution of the time-dependence temperature within the gas layer adjacent to the solid interface

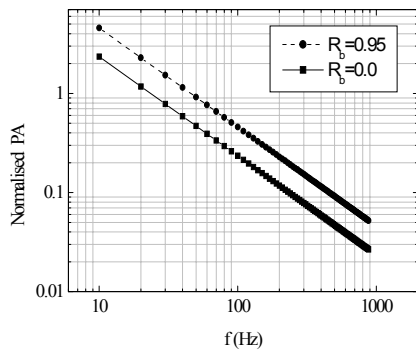


Fig. 4 : Normalised PA signal as function of the modulation frequency of the luminous source.

## DEFECT CHIMISTRY OF TERNARIES

The ternary compounds have a chalcopyrite structure at lower temperatures but show both atomic as well as electronic disorders at high temperatures [5]. In addition, they can have deviations from the ideal molecularity and the valence stoichiometry [4, 5]. Neglecting the cation-

spatial distribution of the temperature in the anion antisite disorders because of their high formation energies, to holes  $h^*$ , and electrons  $e'$ , the intrinsic defects in different charge states that are expected to be formed in the ternary compounds of the type  $A^I B^{III} C_2^{VI}$  are:

$$A_i^+, B_i^{(3-j)^-}, C_i^{(2-k)^-}, V_A^-, V_B^{(3-j)^-}, V_C^{(2-k)^-}, et A_B^{(2-k)^-} \quad (3)$$

Here  $j=0,1$  and  $2$ ;  $k=0$  and  $1$ .

The concentration of all these point defects due to atomic and electronic disorders, in thermodynamic equilibrium, can be calculated by the resolution of the reaction equations as a function of the compound activity [6]. However, it is a very difficult task because of the elevated number of the possible defects in the ternary compound. Using this approach, Groenink and Janse [4] by studying the defect chemistry of ionic ternary compounds consisting of two cations and one anion have determined the conditions for the existence of the majority defect pairs in terms of the crystal composition. According to this model the deviation of their present composition from the ideal formula  $A^I B^{III} C_2^{VI}$  can be described by two parameters  $\Delta x$  and  $\Delta y$ , which determine the deviations from molecularity and valence stoichiometry, respectively. They are defined as :

$$\Delta x = \frac{|A|}{|B|} - 1 \quad (4)$$

$$\Delta y = \frac{2|C|}{|A| + 3|B|} - 1$$

where  $|A|$ ,  $|B|$ , and  $|C|$  are the total concentrations of A, B, and C atoms, respectively, in the compound. An excess of the  $A_2 C^{VI}$  binary compound over  $B_2^{III} C_3^{VI}$  give  $\Delta x > 0$ , whereas an excess of the  $B_2^{III} C_3^{VI}$  binary compound over  $A_2 C^{VI}$  give  $\Delta x < 0$ .  $\Delta y$  determines whether there is an excess or deficiency ( $\Delta y > 0$  or  $\Delta y < 0$ ) of the anions over the cations. The electric activity of the defect in the ternary compound  $A^I B^{III} C_2^{VI}$  are determined from the deviations of the molecularity and the stoichiometry of valence. it is given in the Table I.

Table 1: Electrical activity of defects in  $A^I B^{III} C_2^{VI}$  compounds in dependence on  $\Delta x$  and  $\Delta y$ .

$\Delta x$	$\Delta y$	dominant defect	electrical activity
1	$< 0$	$V_C$	donor (in ionic model ) acceptor (in covalent model )
	$> 0$	$C_i$	acceptor (in both models)
$< 1$	$< 0$	$B_i, B_A$	donor (in both models)
	$> 0$	$V_A$	acceptor (in both models)
$> 1$	$< 0$	$A_i$	donor (in both models)
	$> 0$	$V_B, A_B$	acceptor (in both models)

CIT with only one exception, has always been grown as p-type. From the electrical measurement a shallow level around 15 meV has been reported [5]. The published data of partial vapour pressure below the melting point of different compounds indicates that samples grown from the melt possess a deviation from both molecularity and valence stoichiometry characterised by  $\Delta x < 0$  and  $\Delta y < 0$ . According to Table I the majority defects which can be formed are due to  $Cu_{In}$ ,  $V_{In}$ ,  $In_i$ ,  $Cu_i$ ,  $In_{Cu}$  and  $V_{Te}$  [5].

Electrical properties of CIT have always been measured of samples p-type conducting. It is lucid while using the theory of the covalent bonding model, where the group VI vacancies act as acceptors. However, we should mention that regions n-type conducting have been detected in as-grown ingots of CIT. From which we can conclude that concentration values of Cu interstitial  $N(Cu_i)$  and of Te vacancies  $N(V_{Te})$  are near in their behaviour. This assumption is supported by published data concerning the influence of etch in an atmosphere of copper on the electrical parameters of CIT single crystals [5]. These measurements have established that the concentration of holes is not essentially changed during the etching procedure. But, it has been observed that an increase in the degree of compensation occurred and therefore in the total concentration of donors and acceptors. If we assume that Cu interstitial and Te vacancies are the predominant intrinsic defect formed during etching procedure. we can conclude that the quantity of production of these two defects is nearly equal. But the inequation  $N(V_{Te}) \geq N(Cu_i)$  always remains valid. It is clear that, some electrical and optical studies are necessary to understand the chemical defect origin in CIT and also to determine their activity energies.

### RESULTS AND DISCUSSION

Photoacoustic spectra as function of the photon energy as measured from p-type conducting samples of  $CuInTe_2$  single crystals are shown in Figs. 5, 6, and 7. The spectra show clearly the direct nature of the band to band transition edge together with peaks at lower energies which are associated with transitions between defect states and the conduction/valence bands.

Figs. 8, 9, and 10 show the absorption coefficient spectra of deduced from PA spectra as function of the photon energy at room temperature. The abrupt variation corresponds to the band gap limit  $E_g \approx 0.97 eV$ . The different peaks observed at higher photon energies indicates the existence of many intrinsic defect levels.

The analysis of data indicates that the relation which can describe the absorption spectra near the band gap for  $h\nu > E_g$  is expressed with the formula :

$$(\alpha h\nu)^2 = (h\nu - E_g) \quad (5)$$

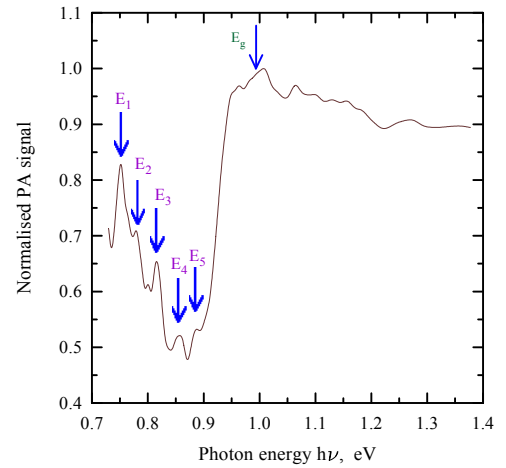


Fig. 5: Photon energy distribution of the normalised PA signal as measured of sample 1.

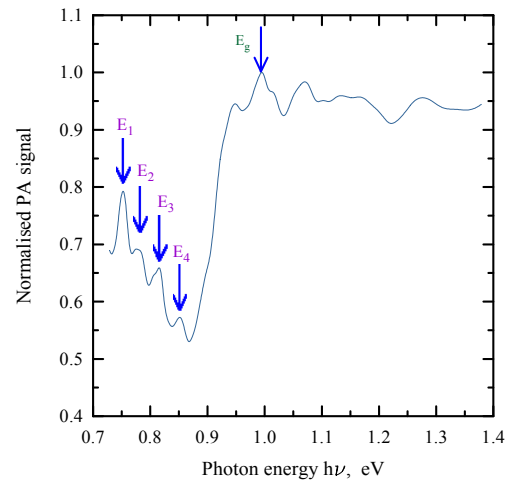


Fig. 6 : Photon energy distribution of the normalised PA signal as measured of sample 2.

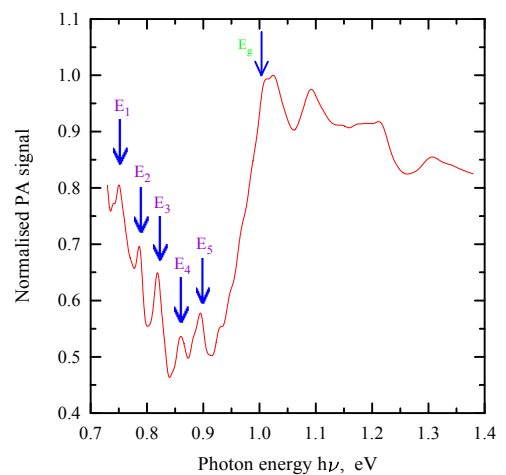


Fig. 7 : Photon energy distribution of the normalised PA signal as measured of sample 3.

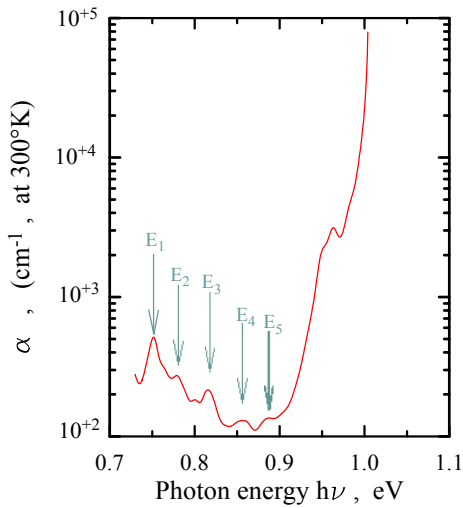


Fig. 8: The spectral dependence of the absorption coefficient calculated from Fig. 5 for the case of sample 1.

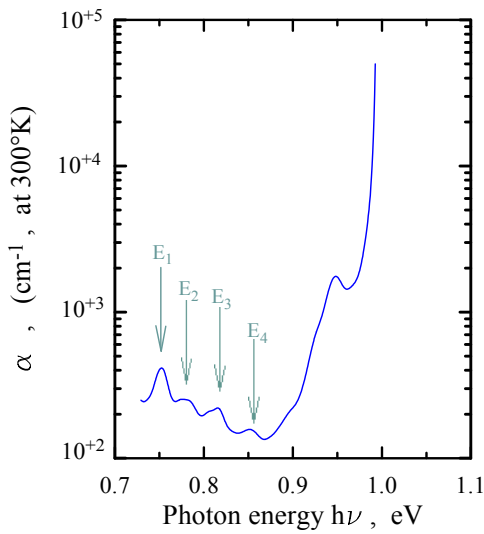


Fig. 9: The spectral dependence of the absorption coefficient calculated from Fig. 6 for the case of sample 2.

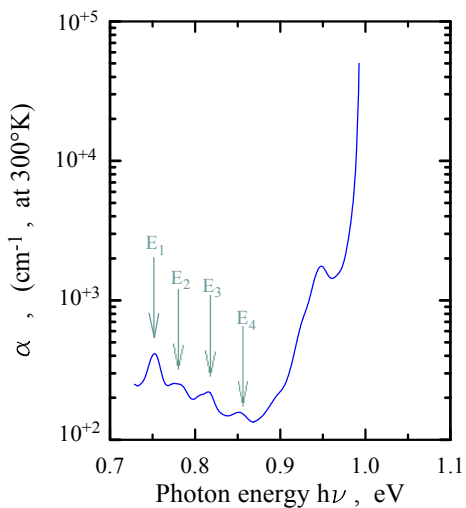


Fig. 10: The spectral dependence of the absorption coefficient calculated from Fig. 7 for the case of sample 3.

From PA spectra, and the absorption coefficient spectra near the fundamental edge, it is clearly observed that CIT is a direct semiconductor with a direct gap. Figs. 11, 12, and 13 show variations of  $(\alpha h\nu)^2$  as a function of the photon energy. From these figures the energy gap of different samples is determined.

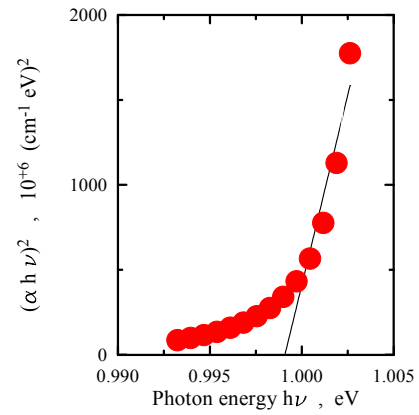


Fig. 11: Plot of  $(\alpha h\nu)^2$  as a function of the photon energy  $h\nu$  for sample 1.

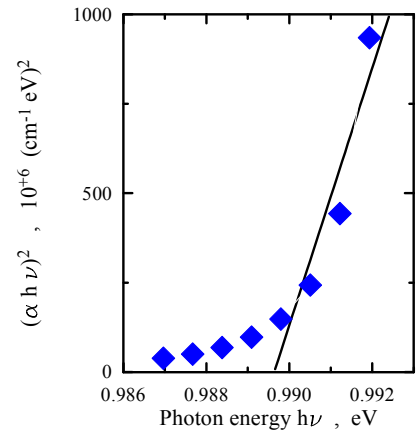


Fig. 12: Plot of  $(\alpha h\nu)^2$  as a function of the photon energy  $h\nu$  for sample 2.

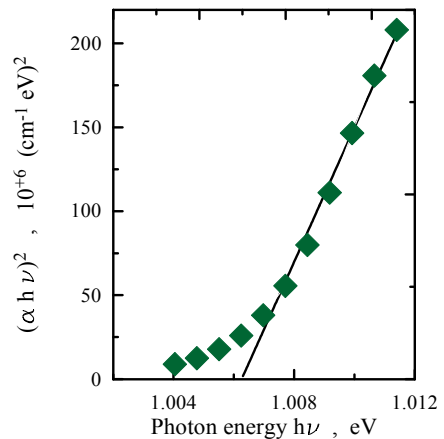


Fig. 13: Plot of  $(\alpha h\nu)^2$  as a function of the photon energy  $h\nu$  for sample 3.

Analysis of the experimental data shows that for all samples the linear portion of the plots is due to an allowed direct transition.

Ionisation energies of intrinsic defects are derived from the appropriately determined values of the gap energy. The values found are given in Table 2 with values of ionisation energies for intrinsic defect states as reported in the literature.

Table 2 : Defect ionisation energies and the energy gap.

	S-1	S- 2	S- 3	Literature
Eg (eV)	0.996	0.989	1.015	0.93-1.06
E1 (meV)	245	237	265	250 [3]
E2 (meV)	218	214	229	200 [13]
E3 (meV)	181	174	197	135-150 [3]
E4 (meV)	139	138	155	-
E5 (meV)	109	-	121	75-90 [3,7]

Different energy levels have been observed in CIT after electrical measurements. The shallow level 15 meV assigned to the antisite defect  $\text{Cu}_{\text{In}}$  [3, 5], the levels 75 meV and 60 meV assigned to the vacancies of Cu ( $V_{\text{Cu}}$ ) and to the vacancies of Te ( $V_{\text{Te}}$ ), respectively [12, 13]. Photoconductivity studies has revealed the existence of two donors levels  $E_D=45$  meV (Neumann and al.), and  $E_D=16$  meV [5]. In general, the conductivity p-type is always governed by the superficial acceptors possessing an ionisation energy that varies in the interval  $E_A=10-25$  meV. Yakushev et al. [13] have identified the existence of deep energy levels where their values vary in the intervals (75-90 meV), (135-150 meV), and (350-500 meV). These values are in good agreement with the values measured in this paper. comparison between values found here and those published in the literature indicate that photoacoustic spectroscopy can be used as a reliable method to reveal the presence of populations of deep defects in CIT and others ternary compounds.

### CONCLUSION

Photoacoustic spectroscopy has been used successfully in the study of the optical properties of p-type conducting  $\text{CuInTe}_2$  single crystals. Shallow

and deep non-radiative transitions have been detected. The gap energy has been determined and is found to be around 0.99 eV with an estimated error in precision of  $\pm 5\%$ . The defect ionisation energies of the defect populations observed in the absorption tail are found to be comparable to those published in the literature. However, the interpretation of the data in term of specific defect states remains speculative and further systematic work is required with single crystal substrates in order to distinguish between surface and bulk states and their effects on optoelectronic characteristics.

### REFERENCES

- [1] M. A. Contreras, B. Egaas, K. Ramanathan, J. Hiltner, A. Swartzlander, F. Hasoon and R. Noufi, Prog. in Photovolt. : Res. and Appl. **7** (1999) 311.
- [2] A. Zegadi, A. Bouloufa, N. Mazouz, B. Barka, E. Ahmed, R. D. Pilkington, A. E. Hill and R. D. Tomlinson, PV in Europe, Rome (Italy) 7 – 11 Oct. (2002)pp. 83-86
- [3] L. I. Haworth, R. D. Tomlinson and I. S. Al-Saffar, Jpn. J. Appl. Phys. **19-3** (1980) 77.
- [4] J. A. Groenik and P. H. Janse, Z. Phy. Chem. **110** (1978) 17.
- [5] C. Rincon and S. M. Wasim, in Ternary and Multinary Compounds, S. K. Deb et al. Eds., MRS (1987) p. 443.
- [6] H. Neumann, Cryst. Res. Technol. **18** (1983) 483.
- [7] B. J. Fernandez, R. Dávila and E. Belandria, Inst. Phys. Conf. Ser. N°152, Section G, Magnetic Materials (1998).
- [8] A. Rosencwaig and A. Gersho, J. Appl. Phys. **47** (1976) 64.
- [9] H. Neumann, Cryst. Res. Technol. **29** (1993) 73.
- [10] A. Zegadi, M. A. Slifkin, M. Djamin, R. D. Tomlinson and H. Neumann, Sol. Stat. Commun. **83** (1992) 591.
- [11] A. Zegadi, M. A. Slifkin and R. D. Tomlinson, Rev. Sci. Instrum. **65** (1994) 2238.
- [12] C. Rincon, S. M. Wasim, G. Marin and G. Sanchez Perez, J. Appl. Phys. **82** (1997).
- [13] M. V. Yakushev, H. Neumann and R. D. Tomlinson, Cryst. Res. Technol. **30** (1995) 121.